RSC Advances

ROYAL SOCIETY OF CHEMISTRY

www.rsc.org/advances

In vivo SAR and STR analyses of alkaloids from *Picrasma quassioides* identify 1-hydroxymethyl-8-hydroxy-*β*-carboline as a novel natural angiogenesis inhibitor

Guiyi Gong[1, §], Qinghua Lin[1, §], Jian Xu[1], Feng Ye[1], Lingling Jiang[2], Wenyuan Liu[3, 4], Ming-Fang He[2], Feng Feng[1, 5, *], Wei Qu[1, *], Ning Xie[6]

[1]Department of Natural Medicinal Chemistry, China Pharmaceutical University, Nanjing 210009, China

[2]Institute of Translational Medicine, College of Biotechnology and Pharmaceutical Engineering, Nanjing Tech University, Nanjing 211800, China

[3]Department of Pharmaceutical Analysis, China Pharmaceutical University, 24 Tongjiaxiang, Nanjing 210009, China

[4]Key Laboratory of Drug Quality Control and Pharmacovigilance (China Pharmaceutical University), Ministry of Education, China Pharmaceutical University, 24 Tongjiaxiang, Nanjing 210009, China

[5]Key Laboratory of Biomedical Functional Materials, China Pharmaceutical University, Nanjing 211198, China

[6]State Key Laboratory of Innovative Natural Medicines and TCM Injections, Jiangxi Qingfeng Pharmaceutical Co., Ltd. Ganzhou 341000, Jiangxi, China

* Corresponding author

Professor Feng Feng: Tel/Fax 86 25 86185216, E-mail: fengfeng@cpu.edu.cn

Dr. Wei Qu : Tel/Fax 86 25 86185216, E-mail: popoqzh@126.com

§ These authors contributed equally to this work.

Abstract:

Angiogenesis plays an important role in the development of inflammatory diseases, including cancer, psoriasis and rheumatoid arthritis. In this paper, we conducted a zebrafish bioassay-guided fractionation of *Picrasma quassioides* and identified twenty alkaloids from the anti-angiogenic fraction, including four new ones (**1 - 4**). In addition, *in vivo* relationships analyses of the structure and anti-angiogenic activity/toxicity led to a conclusion that the skeleton of alkaloids as well as positions and property of the substituents are pivotal to their activity and toxicity. Furancanthin (**1**) is the first-reported furan-fused canthin-6-one with an unprecedented highly-conjugated pentacyclic skeleton. 1-hydroxymethyl-8-hydroxy-*β*-carboline (**3**) was found to have the most potent anti-angiogenic activity and the lowest toxicity *in vivo*, whose anti-angiogenic activity was also confirmed *in vitro*. Further qRT-PCR analysis revealed that the *kdr*, *kdrl* signaling axle in VEGF-VEGFR pathway and the *angpt2b*, *tek* in ANGPT-TEK pathway seemed to be involved in the anti-angiogenic activity of compound **3**.

Introduction

Angiogenesis is a complex process in which several key steps are involved. Although angiogenesis is essential for normal physiological processes, it also plays an important role in the development of inflammatory diseases, including cancer, psoriasis and rheumatoid arthritis.[1] Growing evidence proved that chronic inflammation and angiogenesis are codependent, involving increased cellular infiltration and proliferation as well as overlapping of regulatory growth factors and cytokines.[2] Thus, anti-angiogenic strategy is emerging as an important approach for the treatment and prevention of chronic diseases.[3]

Picrasma quassioides (D.Don) Bennet, which tastes extremely bitter, is one of the most cited species in ancient Chinese medical treatise for a wide range of indications. Its twigs and barks are registered in present Chinese and Asian pharmacopoeias. Therefore, *P. quassioides* is traded across China and usually prescribed as agents in cases of acute colic of gastrointestinal sphere with or without diarrhea. But in Nepal, the extract of *P. quassioides* is applied to treat some intractable skin diseases (such as psoriasis and pruritus) and has significant efficacy.[4]

Previous studies have shown that *P. quassioides* contains a diverse range of bioactive phytochemicals, including alkaloids (*β*-carbolines and canthin-6-ones)[5,6,7], quassinoids[8] and triterpenoids[9]. Nowadays, plenty of researches showed that the alkaloids from *P. quassioides* manifested potent anti-inflammatory effect[10,11,12] and attracted our attention. In addition, many anti-inflammatory herbal medicines (such as *Tripterygium wilfordii*[13,14] and *Alpinia oxyphylla*[15]) and natural products (such as indirubin[16] and rhubarb[17]) showed considerable anti-angiogenic activities, which

might serve as promising drug candidates for the treatment of diseases with abnormally activated angiogenesis. Therefore, it is conceivable that *P. quassioides* and its alkaloids possess potential anti-angiogenic properties. Although *β*-carbolines and canthin-6-ones have been reported to have promising anti-inflammatory activities[10,11,12], the effect of these alkaloids on angiogenesis remains unclear. Only two recent studies touched on the anti-angiogenic effect of one *β*-carboline alkaloid, harmine.[18,19] Moreover, it remains unclear that the relationship between the chemical structure diversity of *β*-carboline alkaloids and the corresponding anti-angiogenic activity.

In recent years, *in vivo* chemical screening in zebrafish (*TG(flia:EGFP)*) has emerged as an ideal method to study anti-angiogenic substances and identify promising lead compounds.[20,21,22,23,24] Moreover, by performing this method, researchers could not only determine the bioactivity and toxicity against the vasculature development in zebrafish embryos, but also conduct structure-activity and structure-toxicity relationships (SAR and STR) studies.[25] In this report, we carried out a phytochemical investigation into the bio-active fraction and the constitutive *β*-carboline alkaloids, then their SAR and STR on anti-angiogenesis were also discussed using *in vivo* zebrafish model. Finally, the action mechanism of a novel *β*-carboline alkaloid, which had the best therapeutic window, was evaluated.

Results and discussion

Bioassay-guided fractionation and structure elucidation

We used zebrafish as a front-line *in vivo* assay model for the bioassay-guided fractionation of crude extracts of *P. quassioides*. We excitedly found that an alkaline (pH-9) fraction which mainly contains alkaloids showed noteworthy anti-angiogenic activity (Fig. S7), prompting us to elucidate its bio-active ingredients. We then conducted a phytochemical investigation into the bio-active fraction and obtained twenty alkaloids, including four new ones (**1 - 4**) (Fig. 1). Herein, we describe the structure elucidation of the four new compounds.

Compound **1** was obtained as white floc. Its molecular formula was established as $C_{17}H_{10}N_2O_3$ from the positive-mode HR-ESI-MS ion at *m/z* 291.0767 $[M+H]^+$ (calcd $[C_{17}H_{10}N_2O_3+H]^+$, 291.0764), indicating 13 degrees of unsaturation. The ^1H NMR spectrum (Table 1) of **1** displayed six well-splitted aromatic proton signals (δ_H 7.29, 7.58, 7.77, 8.28, 8.36, 8.56 and 8.84) that possess 5.7 *Hz*, 8.1 *Hz* coupling constants, one hydroxymethyl signal (δ_H 4.71, 2H d and 5.81, 1H t) and one olefinic proton (δ_H 7.29, 1H s), suggested the canthinone-type skeleton for **1**. The ^{13}C NMR spectrum (Table 1) showed 17 carbon resonances, and aided by HSQC experiments, we categorized them into one methylene (δ_C 56.1); seven methines, and nine quaternary carbons including three oxygenated aromatic carbons or carbonyl carbons (δ_C 145.2, 150.6, 163.9), collectively corresponding to the molecular formula $C_{17}H_{10}N_2O_3$. Then we confirmed **1** as a canthin-6-one instead of a canthin-4-one on the basis of comparison with NMR data of reported drymaritin.[26] Furthermore, compared with those of 5-hydroxymethylcanthin-6-one,[27] which possessed 11 degrees of unsaturation, we noticed that a downshift of olefinic proton of **1** from 8.02 to 7.29. Additionally,

two other quaternary carbons and unsaturation appeared. The key HMBC correlations (Fig. 2) from CH_2-1' (δ_H 4.71) to C-4 (δ_C 163.9) and C-5a (δ_C 103.4), from OH (δ_H 5.81) to C-1' (δ_C 56.1) and C-4 (δ_C 163.9), from olefinic proton (δ_H 7.29) to C-4a (δ_C 145.2), C-4 (δ_C 163.9) and C-5 (δ_C 132.0) revealed a hydroxymethylfuran group in **1**, which might contributed to the extra quaternary carbons and unsaturation. Notably, the correlations from H-1 (δ_H 8.28) to C-4a (δ_C 145.2) and from H-2 (δ_H 8.84) to C-5 (δ_C 132.0) in HMBC experiments can lead to the presence of hydroxymethylfuran group, and the disconnection of oxygenated aromatic carbon and carbonyl carbon. Thus, **1** was determined as 4-hydroxymethyl-canthin [4,5-b]furan-6-one, named furancanthin, which is the first-reported furan-fused canthin-6-one with an unprecedented pentacyclic high-conjugated skeleton.

Compound **2** was isolated as yellow amorphous powder. Its HR-ESI-MS showed an $[M + H]^+$ ion at *m/z* 267.0765 (calcd $[C_{15}H_{10}N_2O_3+H]^+$, 267.0764), indicated a molecular formula of $C_{15}H_{10}N_2O_3$, which possesses 11 indices of hydrogen deficiency. The ^{1}H NMR spectrum (Table 1) of **2** exhibited the resonances of one methoxy group (δ_H 3.99, 3H s), one reactive proton (δ_H 11.02, OH s), five aromatic proton (δ_H 7.02, 7.57, 7.95, 7.98 and 8.72) and one olefinic proton (δ_H 7.40, 1H s), suggesting the presence of a one-substituted carboline-type moiety. The ^{13}C NMR (Table 1) and HSQC data revealed the presence of one methoxy (δ_C 56.5); six methines and eight quaternary carbons including three oxygenated aromatic carbons or carbonyl carbons (δ_C 153.5, 154.3, 154.8), implied a canthinone core skeleton. Compared the spectral data of **2** to those of 5-methoxycanthin-6-one,[28] we easily found that they were quite

similar except for a oxygenated-aromatic carbon. The correlations (Fig. 2) from OCH_3 (δ_H 3.99) to C-5 (δ_C 153.5), from olefinic proton (δ_H 7.40) to C-6 (δ_C 154.3), C-15 (δ_C 126.0) and C-16 (δ_C 135.5), from OH (δ_H 11.02) to C-11 (δ_C 154.8), C-12 (δ_C 112.3) and C-13 (δ_C 139.4), from aromatic proton (δ_H 7.57) to C-11 (δ_C 154.8) and C-13 (δ_C 139.4) observed in HMBC confirmed the location of methoxy group was at C-5 while OH group at C-11. Therefore, the structure of **2** was determined as 11-hydroxy-5-methoxycanthin-6-one.

Compound **3** was obtained as brown needle. The molecular formula was established as $C_{12}H_{10}N_2O_2$ based on its HR-ESI-MS $[M - H]^-$ ion peak at *m/z* 213.0650 (calcd $[C_{12}H_{11}N_2O_2\text{-}H]^-$, 213.0659). The 1D NMR and HSQC spectroscopic data of **3** (Table 2) suggested its *β*-carboline skeleton and displayed one hydroxymethyl group, one hydroxy group. The comparison of the NMR data between **3** and 1-hydroxymethyl-*β*-carboline (**9**) revealed an extra hydroxy group in **3**, which was also confirmed by its molecular formula.[29] The small sample size of **3** prevented acquisition of a ^{13}C NMR spectrum with adequate signal to noise ratio. But HMBC correlations (Fig. 3) from CH_2 (δ_H 4.99) to C-1 (δ_C 145.4) and C-9 (δ_C 133.4), from aromatic proton (δ_H 6.95) to C-5 (δ_C 112.8), C-8a (δ_C 131.1) and C-8 (δ_C 144.2), from proton (δ_H 7.07) to C-4b (δ_C 122.7) and C-8 (δ_C 144.2), from OH (δ_H 10.05) to C-7 (δ_C 112.9), C-8 (δ_C 144.2) and C-8a (δ_C 131.1) suggested that the hydroxymethyl group substituted at C-1 while the hydroxy group at C-8. Thus, **3** was established as 1-hydroxymethyl-8-hydroxy-*β*-carboline.

Compound **4** was isolated as yellow syrup. The positive-mode HR-ESI-MS of **4** gave the ion peak at *m/z* 257.0919 (calcd $[C_{14}H_{12}N_2O_3+H]^+$, 257.0921), which was consistent with the molecular formula $C_{14}H_{12}N_2O_3$. The ^1H NMR spectrum (Table 2) displayed signals for NH at δ 11.39, besides, a set of ABX aromatic signals (δ_H 7.12, 1H d, 7.58, 1H m, 7.60, 1H m) indicated the presence of a mono-substituted aromatic A ring of *β*-carboline and the substitutes at C-6 or C-7. The ortho coupled doublets (δ_H 8.31 and 8.39) with smaller coupling constant of 4.7 *Hz* were typical of heteroaromatic protons, H-4 and H-3 of *β*-carboline skeleton. The proton signals (δ_H 1.41, 3H t and 4.48, 2H q) and three carbon signals (δ_C 14.0, 60.4, 165.2) (Table 2) suggested the presence of an ethoxycarbonyl group at C-1. The *β*-carboline ring and ethoxycarbonyl chain accounted for $C_{14}H_{11}N_2O_2$， with an unaccounted HO from the molecular formula $C_{14}H_{12}N_2O_3$. This suggested the possibility of a hydroxy moiety being the missing fragment of **4**.[30] Comparison of the spectral basis between **4** and 6-hydroxy-1-methoxycarbonyl-*β*-carboline showed the location of the OH moiety at C-6.[31] In its HMBC experiments, the correlations (Fig. 3) from aromatic proton (δ_H 7.12) to C-5 (δ_C 105.4), C-8a (δ_C 134.9) and C-6 (δ_C 151.1), from proton (δ_H 7.58) to C-7 (δ_C 118.6), C-4a (δ_C 130.1), C-8a (δ_C 134.9) and C-6 (δ_C 151.1), from proton (δ_H 7.60) to C-4b (δ_C 120.4) and C-6 (δ_C 151.1) fully supported the assignments above. Hence, **4** was assigned as 6-hydroxy-1-ethoxycarbonyl-*β*-carboline.

The known compounds 4,5-dimethoxy-canthin-6-one (**5**),[32] 4-methoxy-5-hydroxy-canthin-6-one (**6**),[32] canthin-6-one (**7**),[28] 1-aldehyde-*β*-carboline (**8**),[33] 1-hydroxymethyl-*β*-carboline (**9**),[29]

β-carboline-1-carboxylic acid (**10**),[30] *β*-carboline-1-propionic acid (**11**),[32] 1-ethoxycarbonyl-*β*-carboline (**12**),[34] 1-formyl-*β*-carboline (**13**),[34] 1,6-dihydroxy-*β*-carboline (**14**),[35] 1-hydroxy-*β*-carboline (**15**),[35] 4-hydroxy-1-methoxycarbonyl-*β*-carboline (**16**),[35] 4-methoxyl-1-methoxycarbonyl-*β*-carboline (**17**),[36] 4,8-dimethoxy-1-vinyl-*β*-carboline (**18**),[28] 1-carbonyl-6-dihydroxy-*β*-carboline (**19**)[35] and 4,5-dimethoxy-10-hydroxy-canthin-6-one (**20**)[7] were identified by comparison of their observed and reported NMR data.

***In vivo* assessment of anti-angiogenic activity and toxicity of isolated alkaloids**

Transgenic zebrafish (*TG(flia:EGFP)*), which can exhibit vasculature-specific expression of enhanced green fluorescent protein (EGFP) within the whole body during embryonic and larval development, is an ideal *in vivo* model for studying anti-angiogenic agents.[37,38] The primary advantages include their high genetic, physiologic, and pharmacologic similarity with humans, as well as the small size, optical transparency, rapid development, and large numbers of their embryos and larvae. Moreover, along with the assessment of bio-activity, the toxicity of a test compound could also be determined by the influence on the embryo development and body integrity. So, the secondary advantage of zebrafish model is that it can distinguish whether the anti-angiogenic activity of a test compound is through a direct vasculature targeting effect or through a secondary effect caused by development blocking which in turn resulted in the decrease of angiogenesis.

Compounds **1**-**20** at various concentrations were tested for their anti-angiogenic activities and toxicities on transgenic zebrafish from 24 hpf to 72 hpf. The lowest observed effect concentration (LOEC) in terms of anti-angiogenesis, totally lethal concentration (LC_{100}), and anti-angiogenic index (AI, $AI=LC_{100}/LOEC$) values were estimated (Table 3). [21, 23, 24, 39]

As the current data showed (Table 3), the structural diversity of these alkaloids and their anti-angiogenic effects/toxicity roughly defined some structure-activity/toxicity relationships. First of all, the alkaloid skeleton (*β*-carboline type or canthinone type) might be crucial in the determination of their structure-activity/toxicity. Most of the tested *β*-carbolines displayed visible anti-angiogenic effects and had satisfactory AI values while few canthin-6-ones exhibited observable phenotype. Only two canthinones (**5** and **6**), showing strong toxicity on zebrafish at low concentration 25 and 5 μM, respectively, inhibited angiogenisis when the larvae were dying. On the contrary, other canthinones, including **1**, **2**, **7**, **20**, manifested no anti-angiogenic effect and little toxicity to the larvae. In addition, we noticed that compound **3**, **4**, **8**, **12**, **15**, **16** and **18** could exhibit different potency and effectiveness of the anti-angiogenic activities on zebrafish when the embryos were alive and with comparable body morphology and structure to those in control groups (in Table 4). All these alkaloids are *β*-carbolines. The survival rate of zebrafish embryos and the anti-angiogenic activity of these compounds at 72 hpf were summarized in Table 4 for better clarification. These findings suggested that canthinone-type skeleton might be inferior to *β*-carbolines with regard to the anti-angiogenic function.

Besides, the position of substituents also exerted a tremendous influence on the activity and toxicity of these alkaloids. For example, substitutions at C-4 and C-5 in canthinones can seemingly modulate toxicity. Compound **5** and **6**, which possess dual substitutions, affected the development of zebrafish embryos and appeared more toxic than the canthinones with mono-substituted or without one. Notably, compound **5** poisoned and killed the larvae at 25 μM while **20** was a safe compound for zebrafish up to 200 μM, suggesting that an additional OH group at C-10 might reduce toxicity. Similarly, the comparison of the anti-angiogenic activity of **4** with **12** (Table 4) could reveal that the substituents at position C-6 also viably resulted in decreased activity and toxicity to zebrafish, which was further confirmed by comparing **14** and **15** (Table 4). Interestingly, the observed increase in anti-angiogenic activity from **9** to **3** indicated that an OH substituent at C-8 might provide a higher chance to prevent vasculature formation.

Finally, we realized that substituents could had a drastic effect on the anti-angiogenic activity and toxicity to zebrafish. For instance, it was presumably that the hydroxy group, wherever substituted at *β*-carboline skeleton, could lower the toxicity to zebrafish while the replacement of a methoxy group might bring about opposite effect, as indicated by **17**, **18** *vs.* **16**. In contrast to *β*-carbolines, canthinone **5** was safer than **6** to zebrafish, which implied that the methoxy group at canthinones exhibited lower toxicity than hydroxy group. However, these substituents' influences on the anti-angiogenic activity remained unknown and were likely dependent on their substituted positions. From the analysis of the anti-angiogenic *β*-carbolines in Table 4,

it could be concluded that an ester group at C-1 was possibly more active and toxic to zebrafish than carbonyl and hydroxy group, which revealed that a suitable substituent at C-1 play a key role in the anti-angiogenic activity. Compound **8** was far more toxic than other carbolines, which indicated that the aldehyde group at C-1 probably increase toxicity.

In summary, our data indicated that the alkaloid skeleton, substitutions at C-4 and C-5 (canthinones), presence of substituents at C-6 (*β*-carbolines) or C-10 (canthinones), variation of substituents at C-1 (*β*-carbolines) could significantly affect the anti-angiogenic activity and toxicity on zebrafish embryos.

Identification of a novel natural *β*-carboline alkaloid as a potent angiogenic inhibitor

Since anti-angiogenic *β*-carbolines' activity and toxicity were codependent, most of their AI values approximately equal to 1. Therefore, of all investigated compounds, which conformed to the "Rule of Five",[40] the most potent anti-angiogenic activity together with the lowest toxicity to zebrafish embryos was compound **3** (Table 3). In the phenotype-based study, we found that **3** could suppress the angiogenesis in zebrafish embryos dose-dependently (Fig.4). **3** affected the formation of ISVs with mild anti-angiogenic activity at 25 μM, and almost completely arrested the growth of ISVs at 75 μM. Due to the significant therapeutic potential of **3** in terms of its largest AI value *in vivo*, we subsequently investigated its anti-angiogenic activity in mammalian model.

Effects of compound 3 on HUVEC proliferation, migration and tube formation *in vitro*.

The potential anti-angiogenic effect of **3** was further verified by Human Umbilical Vein Endothelial Cell (HUVEC)-based assays *in vitro*. Fig.5 shows the mean survival curves obtained with the CCK-8 assay in HUVECs, from which we estimated IC_{50} value was 94.2 ± 1.7 μM. This effect on cell survival was not endothelial cell-specific, since IC_{50} values of **3** in the treatment of several human cancer cell lines were similar to those obtained for HUVEC (results not shown).

Besides, cells migration is a key step shared by both angiogenesis and tumor progression. Fig.6A showed the effects of different concentrations of **3** on endothelial cell vertical migration ability, as determined by Boyden Chamber migration assay. Quantitative determination of the migrated cells showed a significant inhibitory effect of **3** at more than 25 μM (Fig.6B). Additionally, **3** could inhibit HUVEC horizontal migration ability in a scratch-wound assay (Fig.6C), achieving about 40% inhibition at 50 μM (Fig.6D).

Tube formation is also indispensable for angiogenesis. The tubular structure in the treated wells was rather incomplete with fewer branch points and shorter tube length (Fig.7A). **3** showed an inhibitory effect by about 30% and 70% at 50 μM and 100 μM respectively on HUVECs (Fig.7B), which was comparable to the positive control.

All of the *in vitro* results showed that **3** could inhibit the three key steps including proliferation, migration and tube formation of HUVEC involved in the angiogenesis

progress. Interestingly, **3** showed preferentially inhibition to HUVEC migration than proliferation and tube formation.

Molecular mechanism of compound 3 on zebrafish anti-angiogenesis.

In order to explore the anti-angiogenic mechanism of compound **3**, we evaluated the mRNA expression level of angiogenesis related genes (*angpt2b*, *tek*, *vegfaa*, *flt1*, *kdr*, *kdrl*, *fgf2* and *fgfr2*) by performing qRT-PCR assay in zebrafish embryos. After 24 hours of drug treatment at 48 hpf, the expressions of these genes were indicated in Fig.8. The mRNA expression of *angpt2b* and *tek* was consistently reduced in a dose-dependent manner (60% down-regulated at 75 μM). Besides, the expressions of two receptors in VEGF signaling pathway including *kdr* and *kdrl* were also concentration-dependently down-regulated in response to **3** treatment (50% down-regulated at 75 μM respectively). No obvious alterations of the mRNA expression level of other genes could be observed at all tested concentrations of **3**. These data gave us a clue that **3** exerted anti-angiogenic actions possibly *via* down-regulation of both VEGF-VEGFR (*kdr* and *kdrl*) and ANGPT-TIE (*angpt2b* and *tek*) signaling pathways but not FGF/FGFR in zebrafish.

Conclusion

Taken together, we conducted an *in vivo* zebrafish bioassay-guided fractionation approach and successfully obtained twenty alkaloids, including four new ones (**1** - **4**). *In vivo* phenotype-based screening of all the isolates in zebrafish identified a new

alkaloid, **3** (1-hydroxymethyl-8-hydroxy-*β*-carboline), as a sound and effective natural angiogenesis inhibitor. The anti-angiogenic activity of **3** was confirmed by *in vitro* mammalian assays. Moreover, ANGPT-TIE and VEGF/VEGFR signaling pathways were found to be involved in the anti-angiogenic activity in zebrafish model.

We conducted the SAR and STR studies in live zebrafish embryos, which are inherently likely to assess absorption, distribution, metabolism, excretion, and toxicity (ADMET) and identify compounds having favorable physiochemical properties and excellent "drug-likeness". Our results demonstrate that the zebrafish model is a correlative, convenient and complementary platform for pharmaceutical development that incorporates the assessment of a lead compound's *in vivo* bioactivity and selectivity in the early development process.

Our findings bring new and strong evidence that *β*-carboline type alkaloids might serve as promising anti-angiogenic candidates. Further structural modifications of *β*-carbolines are still underway. Since these alkaloids' anti-inflammatory and anti-angiogenic activities were codependent, their relationships will also be explored in the future.

Experimental section

Plant material

The stems of *Picrasma quassioides* were collected in August 2013 from JiangXi Province, China, and identified by Prof. Feng Feng of China Pharmaceutical

University. A voucher specimen (No. 130901) was deposited in the Department of Natural Medicinal Chemistry, China Pharmaceutical University, China.

Animals, cell culture and chemicals

Transgenic zebrafish *Tg (fli-1:EGFP)* were obtained from Model Animal Research Center of Nanjing University. Primary human umbilical vein endothelial cells (HUVECs) were purchased from Lonza (Switzerland) and cultured on endothelial growth medium-2 (EGM-2, Lonza); HUVECs at early passages (passages 2–7) were used in the experiments. All cells were incubated at 37 °C in 5% CO_2 (v/v). SU5416, and dimethyl sulfoxide (DMSO) were purchased from Sigma-Aldrich (St. Louis, MO).

Extraction and isolation

The air-dried stems (30 kg) of *P. quassioides* were extracted with 95% aq. EtOH (3 × 80 L) under reflux for 2 h, and concentrated in vacuum, affording 350g resultant aqueous residues. Then we added 3%-5% hydrochloric acid solution to the extract and adjusted its pH to 1-2. After extracted with $CHCl_3$, we added aqueous ammonia-solution and obtained pH 6, pH 9, acid-insoluble fractions by pH gradient extraction.

The pH 9 fraction (45 g) was subjected to silica gel CC and eluted with CH_2Cl_2-MeOH (50:1-50:50) to give 8 subfractions (9.1-9.8). Fraction 9.2 was subjected to an ODS-MPLC using a gradient elution with MeOH/H_2O (10:90-100:0)

to afford four fractions, and the fourth fraction 9.2.4 was further separated on RP-TLC ($CHCl_3$/MeOH 20:1) to get **18** (4 mg), **20** (3 mg). Purification of fraction 9.3 on Sephadex LH-20 CC using an isocratic elution with $CHCl_3$/MeOH (1:1) to yield **9** (30 mg), **14** (2 mg), **15** (2 mg), **19** (30 mg). Subfraction 9.4 was further purified by repeated silica gel CC and **1** (4.3 mg), **2** (3 mg), **5** (>1 g), **8** (20 mg), **10** (6 mg), **16** (20 mg), **6** (> 2g) was obtained by recrystallized. Fraction 9.5 was subjected to a silica gel CC using a step gradient of $CHCl_3$/MeOH (30:1-8:2) as eluent to furnish five fractions, and the fifth fraction 9.5.5 was purified by Sephadex LH-20 CC eluted with isocratic $CHCl_3$/MeOH (1:1) to give compound **3** (1 mg). The fraction 9.5.4 was purified on semi-RP-HPLC (60% MeOH, 2 ml/min) to yield compounds **4** (5 mg), **13** (3 mg). Subfraction 9.6 (5g) was repeatedly chromatographed over MCI gel (MeOH/H_2O 1:9-7:3), silica gel (CH_2Cl_2/Actone 10:1-6:1), Sephadex LH-20 (CH_2Cl_2/MeOH 1:1), ODS (MeOH/Water 3:7-5:5) to afford **7** (2.5 mg), **11** (6.3 mg), **12** (8 mg), **17** (5 mg). The purity of compounds **1**−**20** was estimated to be greater than 90%, as determined by ^{1}H NMR spectra.

Compound(1): White floc; m.p. 249-251 ℃; IR (KBr) ν_{max} 3273, 2955, 1628, 1604, 1567, 1469, 1326, 1318, 1269, 1216, 1089, 755 cm^{-1}; ^{1}H NMR and ^{13}C NMR data (DMSO-d_6, see Tables 1); HR-ESI-MS *m/z* 291.0767 $[M+H]^+$(calcd $[C_{17}H_{10}N_2O_3+H]^+$, 291.0764).

Compound(2): yellow amorphous powder; IR (KBr) ν_{max} 3277, 1627, 1602, 1568, 1470, 1438, 1328, 1268, 1214, 1105, 1086, 756 cm^{-1}; ^{1}H NMR and ^{13}C NMR data

(DMSO-d_6, see Tables 1); HR-ESI-MS *m/z* 267.0765 (calcd $[C_{15}H_{10}N_2O_3+H]^+$, 267.0764).

Compound(3): brown needle; m.p. 259-260 ℃; IR (KBr) ν_{max} 3125, 2851, 1628, 1497, 1434, 1322, 1238, 1205, 1027, 821, 744 cm^{-1}; ^1H NMR and ^{13}C NMR data (DMSO-d_6, see Tables 2); HR-ESI-MS *m/z* 213.0650(calcd $[C_{12}H_{11}N_2O_2-H]^-$, 213.0659).

Compound(4): yellow syrup; IR (KBr) ν_{max} 3404, 1677, 1612, 1497, 1440, 1277, 1200, 1032, 726 cm^{-1}; ^1H NMR and ^{13}C NMR data (DMSO-d_6, see Tables 2); HR-ESI-MS *m/z* 257.0919 (calcd $[C_{14}H_{12}N_2O_3+H]^+$, 257.0921).

Anti-angiogenic screening of phytochemicals in zebrafish model

Adult zebrafish were kept and raised according to the Zebrafish book guidelines. We used 20 dechorinated 24 hpf-embryos per experimental group in a 24-well plate and incubated with 1ml of embryo water containing various concentrations of drug at 28.5 °C for additional 48 h. In order to evaluate the compounds' activities in a fast and efficient way, we tested all the compounds at doses of 1, 5, 10, 25, 50, 75, 100, 150, 200μM. After anesthetized with 0.016% tricaine (Sigma-Aldrich), the inter-segmental blood vessels (ISVs) of embryos were observed and imaged at 72hpf under a fluorescence microscope (IX71, Olympus, Japan). SU5416 was served as a positive control. All zebrafish studies were approved by the Institutional Animal Care and Use Committee at Nanjing Tech University.

In vitro proliferation, migration, tube formation assays

All the assays in HUVECs were done following the methods reported previously with some modifications and were described in detail in the Supporting Information.[41, 42]

Reverse transcription, and quantitative real-time PCR

Zebrafish embryos at 24 hpf were treated with 0.1% DMSO and various concentrations of **3** for 24 h. At 48 hpf, total RNA was extracted from 10 zebrafish embryos per treatment group using Trizol Reagent (Invitrogen, USA) according to the manufacturer's protocol. qRT-PCR was performed on the ABI 7900HT Real-Time PCR System (Applied Biosystems, USA) using Taqman probe according to the manufacturer's instructions. The abundance of mRNA was normalized to *gapdh* levels and expressed as percentage of the control (100%) for statistical analysis. The primers were specific for *gapdh* (GenBank ID AF057040), *angpt2b* (AF379603), *tek* (AF053632), *vegfaa* (AF059661), *flt1* (BC163921), *kdr* (DQ026829), *kdrl* (AY056466), *fgf2* (AY269790) and *fgfr2* (AJ309303).

Statistical analysis

All experiments were repeated at least three times. Values are given as means ± the SEM. Data were analyzed using GraphPad Prism 6.0 software (GraphPad Software Inc., La Jolla, CA). Statistical significance was assessed by One-Way analysis of variance (ANOVA) or Student's *t* test. *P* values less than 0.05 were considered statistically significant.

Associated Content

Supporting information: Extensive experimental methods，1D NMR, 2D NMR, HRESIMS spectra of **1**-**4** and bioassay-guided fractionation results are available free of charge via the Internet.

Notes

The authors declare no competing financial interest.

Acknowledgements

This research work was financially supported by the National Natural Science Foundation of China (No. 81573557, No. 81373956 and No.81274064), the Priority Academic Program Development of Jiangsu Higher Education Institutions, the Fundamental Research Funds for the Central Universities (2015ZD010).

References

1. J. Folkman, *Nat. Med.*, 1995, **1**, 27-30.
2. D. H. Paper, *Planta Med.*, 1998, **64**, 686.
3. P. Carmeliet, *Nat. Med.*, 2003, **9**, 653-660.
4. N. P. Manandhar, *Plants and people of Nepal*, Timber Press, Portland, 2002.
5. W. H. Jiao, G. D. Chen, H. Gao, J. Li, B. B. Gu, T. T. Xu, H. B. Yu, G. H. Shi, F. Yang, X. S. Yao and H. W. Lin, *J. Nat. Prod.*, 2015, **78**, 125-130.

6. W. H. Jiao, H. Gao, C. Y. Li, F. Zhao, R. W. Jiang, Y. Wang, G. X. Zhou and X. S. Yao, *J. Nat. Prod.*, 2010, **73**, 167-171.

7. M. X. Jiang and Y. J. Zhou, *J. Asian Nat. Prod. Res.*, 2008, **10**, 1009-1012.

8. S. P. Yang and J. M. Yue, *Helv. Chim. Acta*, 2004, **87**, 1591-1600.

9. Y. Niimi, H. Hirota, T. Tsuyuki and T. Takahashi, *Chem. Pharm. Bull.*, 1989, **37**, 57-60.

10. W. H. Jiao, H. Gao, F. Zhao, H. W. Lin, Y. M. Pan, G. X. Zhou and X. S. Yao, *Chem. Pharm. Bull.*, 2011, **59**, 359-364.

11. H. Fan, D. Qi, M. Yang, H. Fang, K. Liu and F. Zhao, *Phytomedicine*, 2013, **20**, 319-323.

12. F. Zhao, Z. T. Gao, W. H. Jiao, L. P. Chen, L. Chen and X. S. Yao, *Planta Med.*, 2012, **78**, 1906-1911.

13. M. F. He, L. Liu, W. Ge, P. C. Shaw, R. Jiang, L. W. Wu and P. P. But, *J. Ethnopharmacol.*, 2009, **121**, 61-68.

14. M. F. He, Y. H. Huang, L. W. Wu, W. Ge, P. C. Shaw and P. P. But, *Int. J. Cancer*, 2010, **126**, 266-278.

15. Z. H. He, W. Ge, G. G. Yue, C. B. Lau, M. F. He and P. P. But, *J. Ethnopharmacol.,* 2010, **132**, 443-449.

16. D. Alex, I. K. Lam, Z. Lin and S. M. Lee, *J. Ethnopharmacol.,* 2010, **131**, 242-247.

17. Z. H. He, M. F. He, S. C. Ma and P. P. But, *J. Ethnopharmacol.,* 2009, **121**, 313-317.

18. F. Dai, Y. Chen, Y. Song, L. Huang, D. Zhai, Y. Dong, L. Lai, T. Zhang, D. Li, X. Pang, M. Liu and Z. Yi, *PLoS One*, 2012, **7**, e52162.

19. T. P. Hamsa and G. Kuttan, *Eur. J. Pharmacol.*, 2010, **649**, 64-73.

20. L. I. Zon and R. T. Peterson, *Nat. Rev. Drug Discov.*, 2005, **4**, 35-44.

21. J. Hao, J. N. Ho, J. A. Lewis, K. A. Karim, R. N. Daniels, P. R. Gentry, C. R. Hopkins, C. W. Lindsley and C. C. Hong, *ACS Chem. Biol.*, 2010, **5**, 245-253.

22. T. V. Bowman and L. I. Zon, *ACS Chem. Biol.*, 2010, **5**, 159-161.

23. A. Papakyriakou, P. Kefalos, P. Sarantis, C. Tsiamantas, K. P. Xanthopoulos, D. Vourloumis and D. Beis, *Assay Drug Dev. Tech.*, 2014, **12**, 527-535.

24. G. Chimote, J. Sreenivasan, N. Pawar, J. Subramanian, H. Sivaramakrishnan and S. Sharma, *Drug Des. Dev. Ther.*, 2014, **8**, 1107-1123.

25. Y. Peng, J. Li, Y. Sun, J. Y. W. Chan, D. Sheng, K. Wang, P. Wei, P. Ouyang, D. Wang, S. M. Y. Lee and G. C. Zhou, *RSC Adv.*, 2015, **5**, 22510-22526.

26. I. Wetzel, L. Allmendinger and F. Bracher, *J. Nat. Prod.*, 2009, **72**, 1908-1910.

27. T. Ohmoto and K. Koike, *Chem. Pharm. Bull.*, 1984, **32**, 170-173.

28. T. Ohmoto and K. Koike, *Chem. Pharm. Bull.*, 1983, **31**, 3198-3204.

29. Y. Kondo and T. Takemoto, *Chem. Pharm. Bull.*, 1973, **21**, 837-839.

30. Z. Q. Lai, W. H. Liu, S. P. Ip, H. J. Liao, Y. Y. Yi, Z. Qin, X. P. Lai, Z. R. Su and Z. X. Lin, *Chem. Nat. Compd.*, 2014, **50**, 884-888.

31. P. L. Wu, F. W. Lin, T. S. Wu, C. S. Kuoh, K. H. Lee and S. J. Lee, *Chem. Pharm. Bull.*, 2004, **52**, 345-349.

32. T. Ohmoto and K. Koike, *Chem. Pharm. Bull.*, 1984, **32**, 3579-3583.

33. M. Chen, H. Y. Fan, S. J. Dai, and K. Liu, *Chin. Trad. Herb. Drugs*, 2007, **38**, 807-810.

34. J. S. Yang and S. R. Luo, *Acta. Pharm. Sic.*, 1979, **14**, 167-177.

35. W. H. Jiao, H. Gao, C. Y. Li, G. X. Zhou, S. Kitanaka, A. Ohmura and X. S. Yao, *Magn. Reson. Chem.*, 2010, **48**, 490-495.

36. T. Ohmoto, R. Tanaka, and T. Nikaido, *Chem. Pharm. Bull.*, 1976, **24**, 1532-1536.

37. N. D. Lawson and B. M. Weinstein, *Dev. Biol.*, 2002, **248**, 307-318.

38. A. D. Crawford, C. V. Esguerra and P. A. de Witte, *Planta Med.*, 2008, **74**, 624-632.

39. I. K. Lam, D. Alex, Y. H. Wang, P. Liu, A. L. Liu, G. H. Du and S. M. Lee, *Mol. Nutr. Food Res.*, 2012, **56**, 945-956.

40. J. B. Veselinovic, G. M. Kocic, A. Pavic, J. Nikodinovic-Runic, L. Senerovic, G. M. Nikolic and A. M. Veselinovic, *Chem.Biol. Interact.*, 2015, **231**, 10-17.

41. M. F. He, X. P. Gao, S. C. Li, Z. H. He, N. Chen, Y. B. Wang and J. X. She, *Eur. J. Pharmacol.*, 2014, **740**, 240-247.

42. V. Iman, H. Karimian, S. Mohan, Y. H. Hobani, M. I. Noordin, M. R. Mustafa and S. M. Noor, *Drug Des. Dev. Ther.*, 2015, **9**, 1281-1292.

Figure Caption

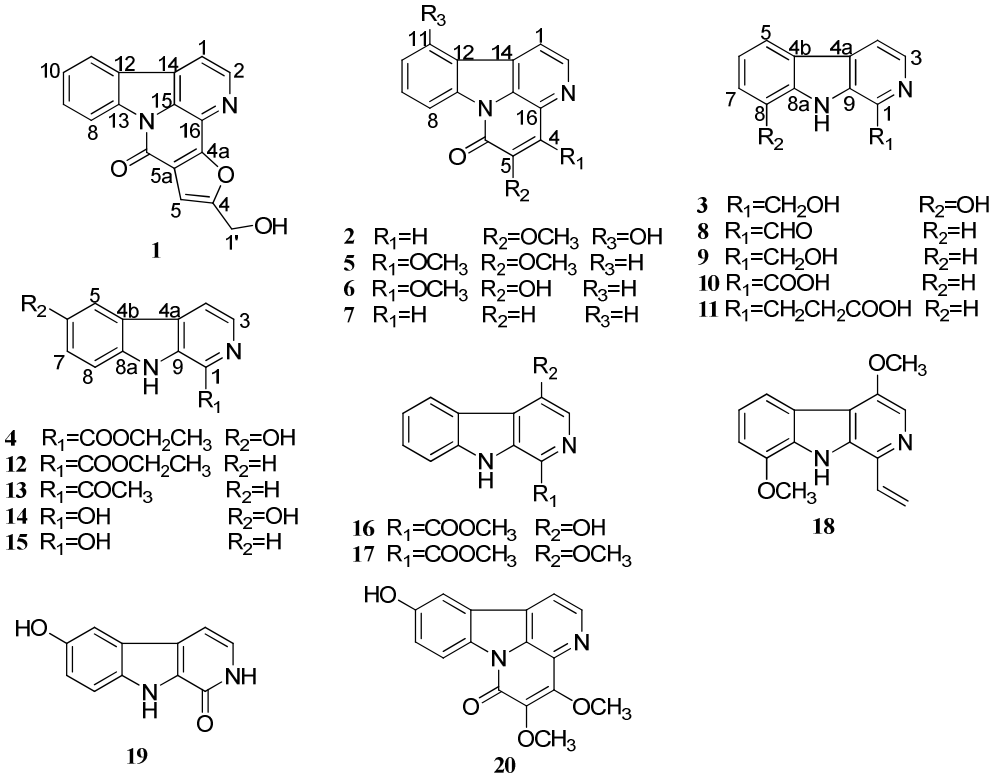

Fig.1. Structures of compounds **1-20**.

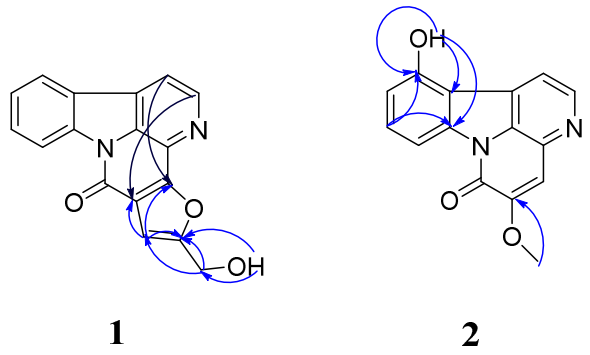

Fig.2. Key HMBC ($^{1}H \rightarrow ^{13}C$) correlations of compounds **1** and **2**.

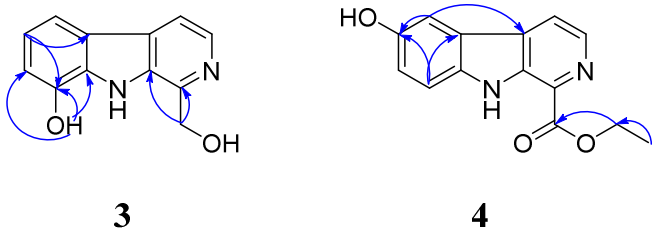

Fig.3. Key HMBC ($^{1}H \rightarrow ^{13}C$) correlations of compounds **3** and **4**.

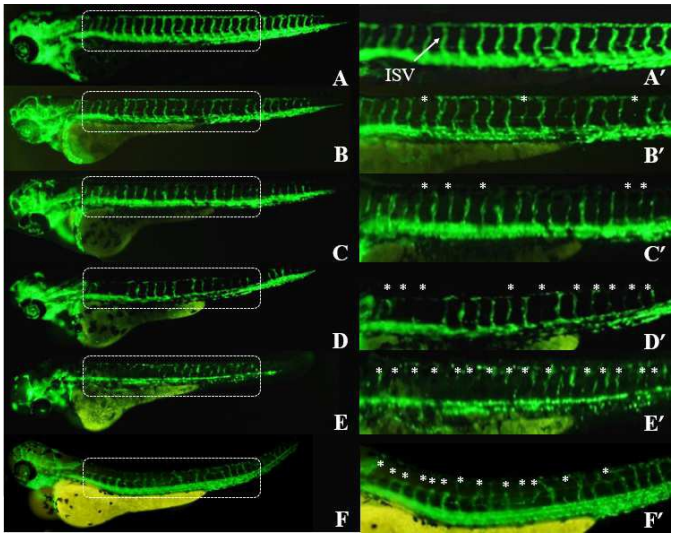

Fig.4. Compound **3** inhibited ISVs angiogenesis in zebrafish. Lateral view of *Tg (fli1:EGFP)* zebrafish embryos at 72 hpf immersed in control (0.1% DMSO), SU5416 (2.5 μM, positive control) and **3** at different concentrations. (A and A') Vehicle-treated control. Arrow indicated EGFP expressing ISVs; (B-E and B'-E') Compound **3** treated embryos at concentrations of 25 μM, 50 μM, 75μM and 100 μM. (F and F') SU5416 treated embryos. Defects in ISVs formation were marked with asterisks. The magnified views of A-F (40X magnification) were shown in A'-F' (100X magnification), respectively.

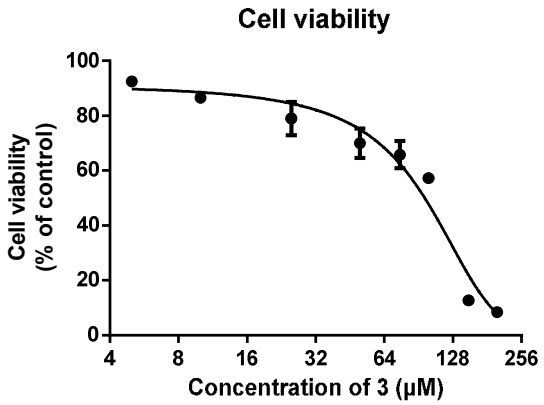

Fig.5. Compound **3** inhibited cell proliferation in HUVECs in a dose-dependent manner under normal culture conditions. Attached cells were treated by various concentrations of **3** for 72 h. Cell growth was quantified by CCK-8 assay. Cells receiving 0.1% DMSO only served as a control. Data were expressed as percentages of the control and as the mean ± S.E.M. of triplicate experiments.

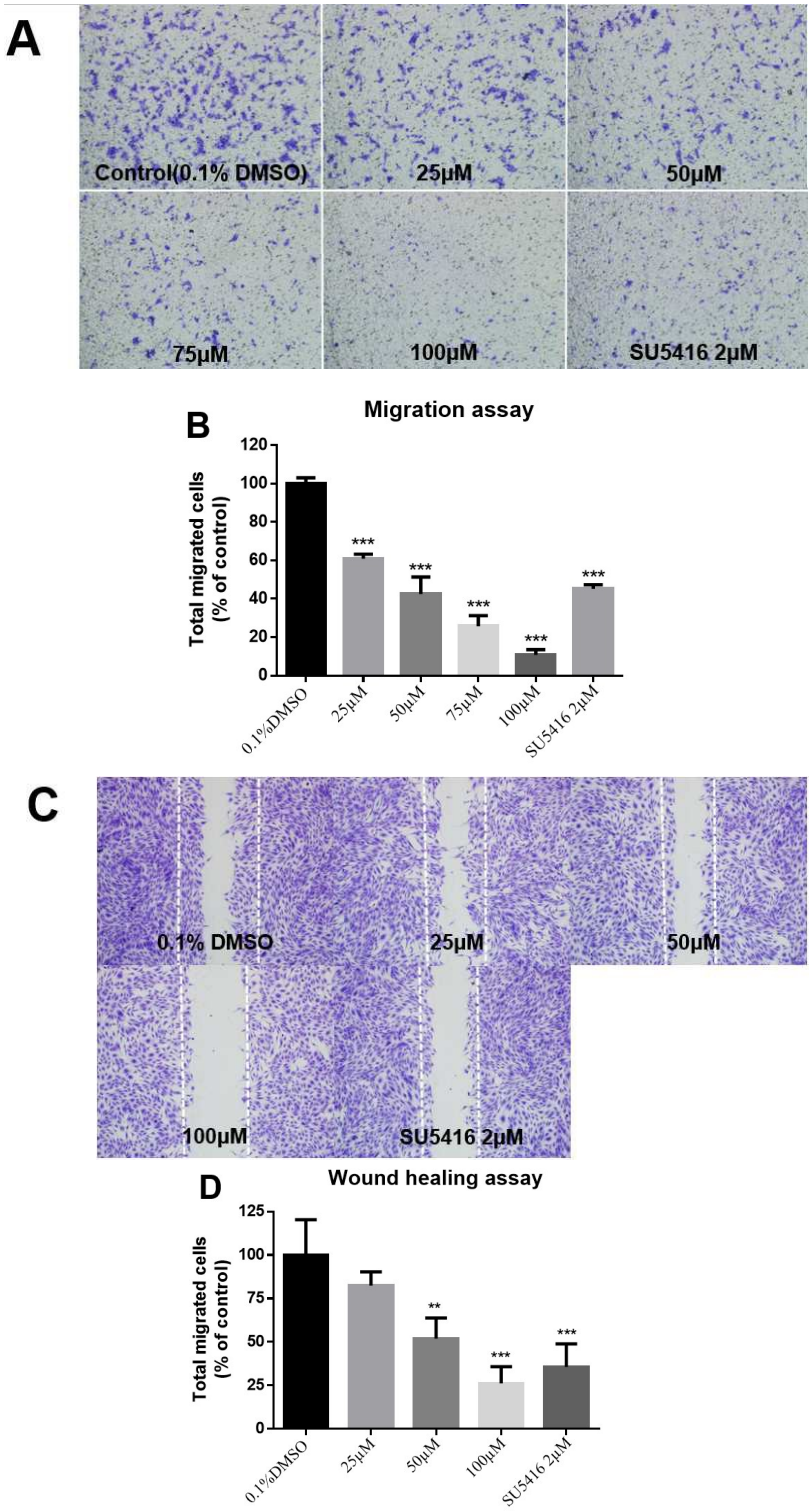

Fig.6. Compound **3** inhibited HUVEC migration by a Boyden chamber migration assay and a scratch-wound assay. (A) A total of 8,000 HUVECs per well were seeded in the

top chamber and treated with 0.1% DMSO only (control), 2 μM SU5416 (positive control) and different concentrations of **3**. (B) After 8 hours, the HUVECs that migrated through the membrane were stained and quantified. (C) Confluent monolayer of HUVECs was wounded (scratched by pipette tips, the wound was shown between the two white dash lines in each photo) at 0 h and then was treated with control, positive control and various concentrations of **3** for 12 h. (D) Quantification of the number of migrated cells (cells between the two white dash lines) after 12 h exposure. For each treatment condition, four measurements were taken randomly in each well of three replicates. Percentage of inhibition was expressed using control wells at 100%. Data was expressed as mean ±S.E.M. of triplicate experiments. Statistical significance was expressed as ***, $P<0.001$; **, $P<0.01$ versus control; one-way ANOVA followed by the Dunnett's multiple comparison tests.

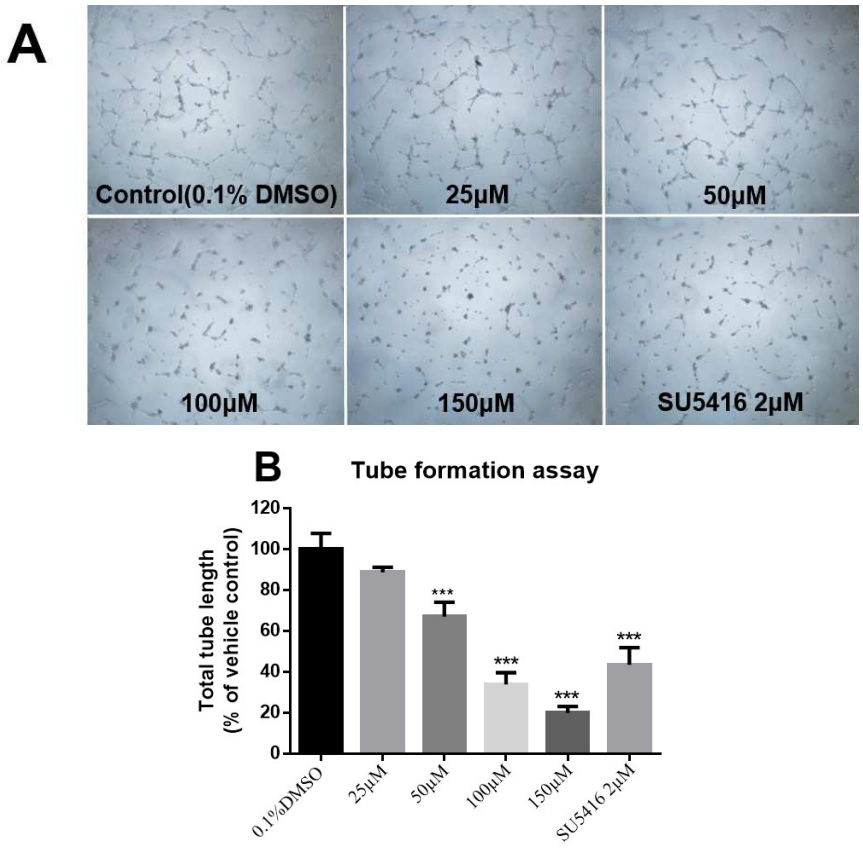

Fig.7. Compound **3** inhibited HUVEC tube formation. (A) Images showing the morphological features of **3**-treated HUVECs on Matrigel. The vessel length decreased after 12 h incubation with **3**. (B) The vessel length in each treatment conditions was quantified. For each treatment condition, four measurements were taken randomly in each well of three replicates. Percentage of inhibition was expressed using control wells at 100%. Data was expressed as mean ± S.E.M. ***，P < 0.001, in one-way ANOVA followed by the Dunnett's multiple comparison test.

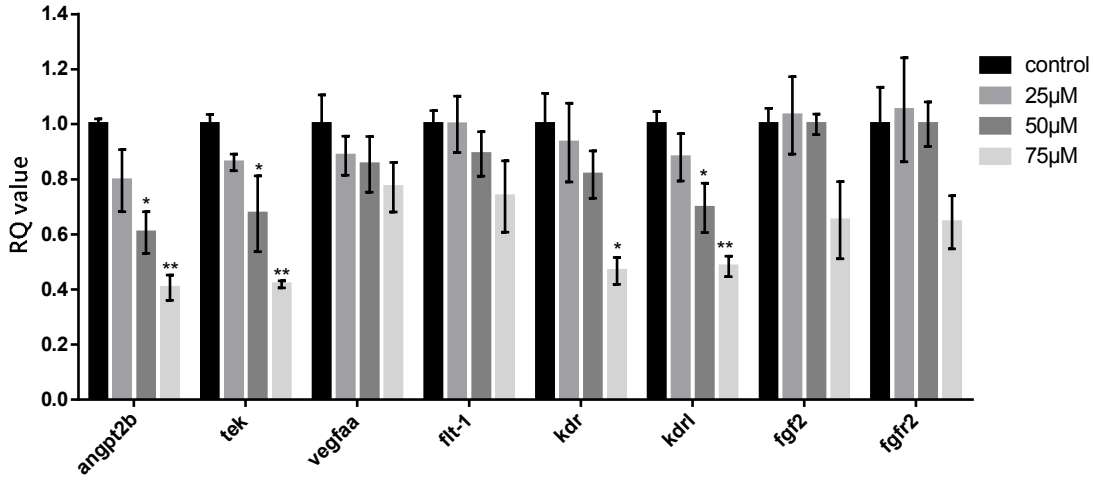

Fig.8. Compound **3** inhibited both VEGF-VEGFR-2 and ANGPT-TIE signaling pathway but not FGF-FGFR-2 on zebrafish. qRT-PCR analysis of these three signaling pathways (*angpt2b, tek, vegfaa, flt-1, kdr, kdrl, fgf2, fgfr2*) mRNA expression in 48 hpf whole embryos treated with various concentrations of **3** or control (0.1% DMSO). Data was expressed as mean ± S.E.M. of triplicate experiments. Statistical significance was expressed as **, $P<0.01$; *, $P<0.05$ versus control; one-way ANOVA followed by the Dunnett's multiple comparison tests.

Table 1. ^{1}H, ^{13}C NMR and HMBC Data for **1** and **2** (300 and 125 MHz, respectively, in DMSO-d_6)

Position	**1**			**2**		
	δ_H mult (*J* in Hz)	δ_C	HMBC（H to C）	δ_H mult (*J* in Hz)	δ_C	HMBC（H to C）
1	8.28 (1H, d, 5.1)	115.9	4a, 12, 14, 15	7.95 (1H, d, 5.1)	115.0	2, 15
2	8.84 (1H, d, 5.1)	145.4	1, 5, 15, 16	8.72 (1H, d, 5.1)	145.6	1, 14
4		163.9		7.40 (1H, s)	109.9	6, 15, 16,
4a		145.2				
5	7.29 (1H, s)	103.4	4, 4a, 5		153.5	
5a		132.0				
6		150.6			154.3	
8	8.56 (1H, d, 8.2)	116.2	11, 12, 13	7.98 (1H, d, 8.1)	107.0	12
9	7.77 (1H, t, 5.7)	130.8	10, 11, 13	7.57 (1H, t, 8.1)	131.6	11, 13
10	7.58 (1H, t, 5.7)	125.4	8, 9, 12, 13	7.02 (1H, d, 8.2)	111.9	8, 12
11	8.36 (1H, d, 8.2)	123.5	8, 13, 14,		154.8	
12		124.8			112.3	
13		138.6			139.4	
14		130.1			127.4	
15		132.4			126.0	
16		129.6			135.5	
1’	4.71 (2H, d, 5.9)	56.1	4, 5a			
1’-OH	5.81 (1H, t, 6.0)		1’, 4			
5-OCH_3				3.99 (3H, s)	56.5	5
11-OH				11.02 (1H, s)		11, 12, 13

Table 2. ^{1}H, ^{13}C NMR and HMBC Data for **3** and **4** (300 and 125 MHz, respectively, in DMSO-d_6)[a]

position	**3**			**4**		
	δ_H mult (*J* in Hz)	δ_C	HMBC（H to C）	δ_H mult (*J* in Hz)	δ_C	HMBC（H to C）
1		145.4			129.2	
3	8.23 (1H, d, 5.3)	136.4	1, 4, 4a	8.39 (1H, d, 4.7)	136.6	1, 4, 4a, 9a
4	8.00 (1H, d, 5.5)	114.5	4b, 8	8.31 (1H, d, 4.6)	118.4	4a, 4b, 9a
4a		129.3			130.1	
4b		122.7			120.4	
5	7.67 (1H, d, 8.1)	112.8	4b, 7, 8a	7.58 (1H, s)	105.4	4a, 7, 8a
6	7.07 (1H, t, 7.8)	120.9	4b, 8		151.1	
7	6.95 (1H, d, 7.5)	112.9	5, 8, 8a	7.12 (1H, d, 8.6)	118.6	5, 8a
8		144.2		7.60* (1H, m)	113.0	4b, 6
8a		131.1			134.9	
9a		133.4			136.1	
1’	4.99 (2H, d, 5.7)	63.3	1, 9a			
1’-OH	5.57 (1H, t, 5.7)		5, 8, 8a			
8-OH	10.05 (1H, s)		7, 8, 8a			
NH	11.09 (1H, s)			11.39 (1H, s)		4a, 4b, 9a
1’-C=O-					165.2	
2’-OCH_2-				4.48 (2H, q, 7.0)	60.4	1’, 3’
3’-CH3				1.41 (3H, t, 7.0)	14.0	2’,

[a]Chemical shifts marked with an asterisk (*) indicate overlapped signals.

Table 3. *In vivo* assessments of the isolated alkaloids in zebrafish[a]

Compound	*C* log P	LOEC (μM)	LC_{100} (Toxicity, μM)	AI
1	2.00	N.d.	N.d.	N/A
2	2.25	>200	>200	1
3	1.54	25	150	6
4	2.39	150	200	1.3
5	2.43	>25	25	<1
6	2.42	>5	5	<1
7	2.27	>200	>200	1
8	2.48	5	10	2
9	1.97	>200	>200	1
10	2.91	N.d.	N.d.	N/A
11	2.32	>200	>200	1
12	2.81	75	150	2
13	2.79	>200	>200	1
14	2.42	>200	>200	1
15	2.85	100	>200	2
16	2.65	100	150	1.5
17	2.66	>10	10	<1
18	3.75	25	50	2
19	0.57	N.d.	N.d.	N/A
20	2.16	>200	>200	1
SU5416	2.83	1	5	5

[a] *C* log P values : Calculated from Chem3D. LOEC: lowest observed effect concentration, it was the treatment concentration that resulted in anti-angiogenic effects on most of the zebrafish larval population; LC_{100} : totally lethal concentration, it was a concentration that resulted in 100% mortality of the embryos during the incubation period; AI: anti-angiogenic index, LC_{100} / LOEC, was considered as the concentration range between LOEC and LC_{100}, it revealed the sub-lethal effects of the compounds with respect to its efficacious concentrations. N.d., not determined due to precipitation. N/A, not applicable. For comparison, the effects of the known KDR inhibitor SU5416 are shown at the bottom. Results from at least 20 embryos per condition.

Table 4. The survival rate (%) and anti-angiogenic effect (+) of seven *β*-carboline alkaloids on zebrafish embryos.

number	concentration （μM）							
	5	**10**	**25**	**50**	**75**	**100**	**150**	**200**
3	100	100	100 (+)	100 (++)	78.3 ± 7.6 (+++)	60.0 ± 15.0 (+++)	0	0
4	100	100	100	100	100	93.3 ± 2.9	83.3 ± 2.9 (+)	0
8	68.3 ± 7.6 (+)	0	0	0	0	0	0	0
12	100	100	100	100	98.3 ± 2.9 (+)	46.7 ± 10.4(++)	0	0
15	100	100	100	100	100	100 (+)	100 (++)	100 (+++)
16	100	100	100	100	100	93.3 ± 7.6 (+)	0	0
18	100	100	82.7 ± 12.6 (+)	0	0	0	0	0

The data are presented as mean ± SEM of at least three individual experiments. + is the estimated arbitrary unit of anti-angiogenic activity of bthe alkaloids. +, mild; ++, moderate; +++, strong.

Graphical Abstract

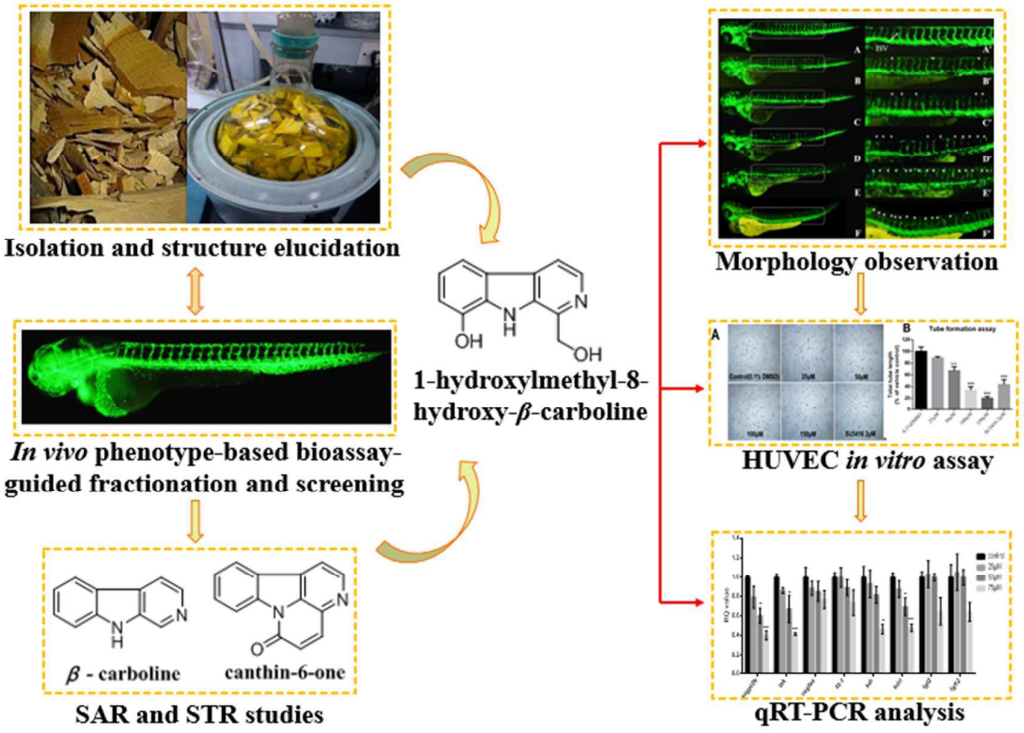

Twenty alkaloids were obtained from the anti-angiogenic fraction of *Picrasma quassioides* and their structure activity and toxicity relationships were studies by an *in vivo* phenotype-based screening. **3** was found to have the most potent anti-angiogenic activity and the lowest toxicity *in vivo* and also confirmed *in vitro*. Finally, the action mechanism of **3**, which had the best therapeutic window, was evaluated by qRT-PCR analysis.